Current Biology Report

Title: A feathered dinosaur tail with primitive plumage trapped in mid-Cretaceous amber

Authors: Lida Xing[1, 2*†], Ryan C. McKellar[3,4*†], Xing Xu[5†], Gang Li[6†], Ming Bai[7†], W. Scott Persons IV[8], Tetsuto Miyashita[8], Michael J. Benton[9], Jianping Zhang[2], Alexander P. Wolfe[8], Qiru Yi[6], Kuowei Tseng[10], Hao Ran[11], Philip J. Currie[8]

Affiliations:

[1] State Key Laboratory of Biogeology and Environmental Geology, China University of Geosciences, Beijing 100083, China
[2] School of the Earth Sciences and Resources, China University of Geosciences, Beijing, 100083, China.
[3] Royal Saskatchewan Museum, Regina, Saskatchewan, S4P 4W7, Canada.
[4] Biology Department, University of Regina, Regina, Saskatchewan, S4S 0A2, Canada.
[5] Key Laboratory of Vertebrate Evolution and Human Origins, Institute of Vertebrate Paleontology and Paleoanthropology, Chinese Academy of Sciences, Beijing 100044, China.
[6] Institute of High Energy Physics, Chinese Academy of Science, Beijing 100049, China.
[7] Key Laboratory of Zoological Systematics and Evolution, Institute of Zoology, Chinese Academy of Sciences, Beijing, 100101, China.
[8] Department of Biological Sciences, University of Alberta, Edmonton, Alberta, T6G 2E9, Canada.
[9] School of Earth Sciences, University of Bristol, Bristol, BS8 1RJ, UK
[10] Department of Exercise and Health Science, University of Taipei, Taipei 11153, China.
[11] Key Laboratory of Ecology of Rare and Endangered Species and Environmental Protection, Ministry of Education, Guilin 541004, China.

*** Contact information:** xinglida@gmail.com (L.X.); ryan.mckellar@gov.sk.ca (R.C.M., lead contact).

[†] These authors contributed equally to this work.

Summary. In the two decades since the discovery of feathered dinosaurs [1–3], the range of plumage known from non-avialan theropods has expanded significantly, confirming several features predicted by developmentally informed models of feather evolution [4–10]. However, three-dimensional feather morphology and evolutionary patterns remain difficult to interpret, due to compression in sedimentary rocks [9,11]. Recent discoveries in Cretaceous amber from Canada, France, Japan, Lebanon, Myanmar, and the USA [12–18] reveal much finer levels of structural detail, but taxonomic placement is uncertain because plumage is rarely associated with identifiable skeletal material [14]. Here we describe the feathered tail of a non-avialan theropod preserved in mid-Cretaceous (~99 Ma) amber from Kachin State, Myanmar [17], with plumage structure that informs directly the evolutionary developmental pathway of feathers. This specimen provides an opportunity to document pristine feathers in direct association with a putative juvenile coelurosaur, preserving fine morphological details, including the spatial arrangement of follicles and feathers on the body, and micrometre-scale features of the plumage. Many feathers exhibit a short, slender rachis with alternating barbs and a uniform series of contiguous barbules, supporting the developmental hypothesis that barbs already possessed barbules when they fused to form the rachis [19]. Beneath the feathers, carbonized soft tissues offer a glimpse of preservational potential and history for the inclusion; abundant Fe^{2+} suggests vestiges of primary haemoglobin and ferritin remain trapped within the tail. The new find highlights the unique preservation potential of amber for understanding the morphology and evolution of coelurosaurian integumentary structures.

Keywords: Coelurosauria; feather evolution; Burmese amber; Cenomanian

Results and Discussion:

Preservation. The tail within DIP-V-15103 is visible to the naked eye as an elongate and gently curved structure (length = 36.73 mm). A dense covering of feathers protrudes from the tail, obscuring underlying details, so Synchrotron Radiation (SR) X-ray phase contrast μCT scanning was employed to examine concealed osteological and soft tissue features (Figure 1). Soft tissues—presumably muscles, ligaments, and skin—are visible sporadically through the plumage, clinging to the bones in a manner suggestive of the desiccation common to other

vertebrate remains in amber [20]. These tissues have largely been reduced to a carbon film, retaining only traces of their original chemical composition. Based on analyses further described in the Supplemental Information, SR μ-XFI shows iron is present in the carbonized soft tissues, and as a series of fine linear features corresponding to exposed plumage (Figure 2). Copper is slightly more abundant in amber containing plumage, but this signal is cryptic and not a clear indicator for preserved pigments. Elements such as Ca, Sc, Zn, Ti, Ge, Mn appear associated with clay minerals filling voids in the amber. We derived the valence state of iron in the sample qualitatively by comparison to the standard XAS of Fe foil, Fe_2O_3, Fe_3O_4, and FeO. Our calculations indicate that more than 80% of iron in the sample is ferrous (Fe^{2+}). Similar measurements have been made on vessels preserved within *Tyrannosaurus* and *Brachylophosaurus* bones, and interpreted as indicating the presence of goethite and biogenic iron oxides produced from haemoglobin decomposition [21]. The presence of large quantities of Fe^{2+} in DIP-V-15103 suggests that some primary iron from haemoglobin or ferritin remains trapped within the inclusion. SEM analyses show pyrite (FeS_2) is also present, but not as a significant contributor to the distribution of iron within the specimen (Figure S3).

The close contact between the skin and surrounding amber, paired with the mummified external appearance of the skin where it has shriveled across the surface of the vertebrae, suggest one of two scenarios. Either the tail-bearer was dead and partially desiccated before encapsulation, or rapidly dried due to resin interactions. Early-stage drying is further supported by the limited amount of cloudy amber surrounding the tail (Figures 1C, S2), which is a preservational feature related to decay products or moisture interacting with resin [22]. However, drying and resin impregnation were not sufficient to preserve cellular detail in the soft tissues. Based on the clays observed where bone breaches the amber surface, skeletal material was likely exposed on the surface after resin polymerization. The bone has been partially dissolved and infilled with clay from the surrounding matrix [17], much like insect body cavities in this deposit (Figure S2A). Presence of Fe^{2+} within the carbonized remains suggests that organic components were trapped early and remained undisturbed by subsequent events. Further taphonomic constraints are difficult to infer. It is unclear whether the lack of melanosomes within the keratin sheets of the surrounding feathers (Figures 2B, S3) might provide additional taphonomic information, or if their absence results from weakly pigmented feathers or the small sample area available for SEM analyses. Artificial maturation experiments [23] have shown the breakdown of

modern melanosomes at a range of temperatures, but this work was conducted at temperatures that would also degrade amber. The taphonomic pathway that led to the preservation of DIP-V-15103 is not entirely clear, but it suggests promise for more detailed examinations of organics or pigmentation in vertebrate inclusions.

Osteology. SR X-ray μCT scanning of DIP-V-15103 (Figure 1) revealed that soft tissues have a density insufficiently different from the partially replaced skeletal elements to permit X-ray imaging and virtual dissection of osteology alone. Consequently, many diagnostic and comparative osteological details remain obscured. However, two vertebrae are clearly delineated ventrally (Figure 1F–H). Extrapolating lengths of these vertebrae, the preserved tail section contains at least eight full vertebrae and part of a ninth. The vertebrae are elongate, with anteroposterior lengths double the maximum diameter of the tail (Supplemental Table 1). Vertebral proportions and tail flexion preclude membership within the Pygostylia [*sensu* 24]. Even with the skin adpressed to the bony surface, no features other than the grooved ventral sulci of two centra are clearly visible. This lack of topography suggests that the vertebrae lack prominent neural arches, transverse processes, or haemal arches. Therefore, the preserved segment is only a small mid to distal portion of what was likely a relatively long tail, with the total caudal vertebral count not reasonably less than fifteen, and likely greater than twenty-five. Based on specimen size, it also seems likely that the tail belonged to a juvenile.

DIP-V-15103 is interpreted as a non-avialan coelurosaur tail: its vertebral profiles and estimated length rule out avebrevicaudan birds, oviraptorosaurs, and scansoriopterygians—lineages generally characterized by a short caudal series with subequal centra [25–27], with the exception of *Epidendrosaurus*. The branched feathers have a weak pennaceous arrangement of barbs consistent with non-avialan coelurosaurs, particularly paravians. Although the feathers are somewhat pennaceous, none of the observed osteological features preclude a compsognathid [28] affinity. The presence of pennaceous feathers in pairs down the length of the tail may point toward a source within Pennaraptora [9], placing a lower limit on the specimen's phylogenetic position. However, the distribution and shape of the feathers only strongly supports placement crownward of basal coelurosaurs, such as tyrannosaurids and compsognathids. In terms of an upper limit, the specimen can be confidently excluded from Pygostylia; and it can likely be excluded from the long-tailed birds, based on pronounced ventral grooves on the vertebral

centra. Additional taxonomic assessment details are provided in Supplemental Information.

Plumage. Both SR X-ray μCT reconstruction and standard light microscopy confirm feather attachments throughout the preserved tail length (Figure 1). A bilaterally paired series of posterodorsally oriented feathers extends from the dorsal midline (Figure 1D,E). Another row of feathers is present at mid-height on each side of the tail, with feathers extending posterolaterally at roughly 45° to its long axis (Figure 1D–G). These follicle pairs appear evenly spaced along the length of the tail. Where the outlines of two vertebral centra are visible, follicles are located at the mid-lengths of centra and at intervertebral joints. Ventral plumage is sparse, consisting of fine feathers that follow the long axis of the tail closely (Figure 1 B,G,H). Overall, the plumage forms laterally directed keels on either side of the vertebral column, providing a unique opportunity to observe feather counts and orientations within the contour-like caudal plumage of a coelurosaur. DIP-V-15103 does not show the splaying of large pennaceous rectrices observed alongside the posteriormost caudals of long-tailed birds [29]. Either splaying was absent in this individual, or only present caudally, beyond the preserved region. Nevertheless, the arrangement of feathers into lateral keels in DIP-V-15103 is similar to the paravian tail fan or frond [9]. Such arrangements, composed of different feather types, can occur not just at the distal tip but also along the entire length of the tail. Amber preservation suggests that the tail fans and fronds preserved in paravians are not merely a taphonomic artefact of compression.

If DIP-V-15103 indeed represents a juvenile coelurosaur tail, the feathers most likely characterize adult plumage—however there is some room for uncertainty. Basal taxa within Pennaraptora, such as *Similicaudipteryx,* are thought to have undergone dramatic moults that affected the tail region [8], meanwhile some basal members of Pygostylia have precocial juveniles with adult-like plumage [14]. The pennaceous feathers and barbules of DIP-V-15103 suggests an adult-like plumage, where feathers would not have been replaced by different morphotypes in subsequent moults. Alternatively, the feather-bearer may not have conformed to the moult patterns found in modern birds.

The feathers of DIP-V-15103 are similar to each other in morphology, regardless of position on the tail (Figures 3, S4). All preserved feathers have a weakly defined rachis that is nearly indistinguishable from the barb rami apically, and slightly thickened basally (Figure 3). Both rachises and barbs are sub-cylindrical in cross section. Although the rachis thickens basally, the

maximum diameter near the follicle is approximately three times that of an adjacent barb ramus (Figures 3, S4). Feathers near the anterior end of the dorsal series have the greatest basal expansion observed among the plumage, with rachis widths approaching 60 μm (Figures 3, 4A,B). Rachises among these feathers become as narrow as 18 μm in apical positions, while barb rami have widths ranging from 15 to 23 μm. Within individual feathers, barbs are positioned alternately along the rachis, approaching an opposite arrangement basally, with wide spacing between, and a weak planar arrangement (Figure 4). Flexion within the amber indicates barb rami were flexible, and the rachis itself was somewhat flexible. The open, flexible structure of these feathers is more analogous to modern ornamental feathers than to flight feathers, showing structural similarities to the distal components of contour feathers in certain Anseriformes (Figures 3, S5). The paired feather arrangement is similar to rectrices in modern birds, suggesting that tracts had become established in basal tail plumage before pygostyle development, with tail plumage becoming more specialized over time. If the entire tail bore plumage similar to that trapped in DIP-V-15103, the feather-bearer would likely have been incapable of flight.

The feathers of DIP-V-15103 display exquisitely preserved barbules. Strikingly, the simple barbules branch not only within individual barbs but also unmodified from the rachis (Figures 3; 4; S4G,H). In this regard, the feathers are comparable to the contours of many modern birds, which also possess some barbules that originate from the rachis (rachidial barbules), although usually from the proximal barb base and in reduced form. In DIP-V-15103, barbules branch in an evenly spaced, paired, and nearly symmetrical manner. This pattern remains consistent in both proximal and distal barbules, from proximal to distal barbs, and along the rachis. Barbules are consistently blade-shaped, with pigmentation outlining five basal cells followed by a poorly differentiated pennulum lacking discernible nodes or nodal protrusions (Figure 3E–H). Close spacing between barbules, combined with the orientation of their flattened surfaces (parallel to the feather's long axis), yields open-vaned feathers that are largely pennaceous.

The weakly developed rachis and contiguous barbule branching in DIP-V-15103 represents a novel combination among theropods. Within the evolutionary developmental model of feathers [5], DIP-V-15103 appears intermediate between stages IIIa (rachis with naked barbs) and IIIb (barbs with barbules, lacking a rachis), but does not exactly fit Stage IIIa+b (rachis with barbs bearing barbules) (Figure 4C). In DIP-V-15103, barbs exhibit an alternating arrangement along a

poorly defined rachis, with nearly dichotomous branching apically, and barbules continue along the surface of the rachis and barbs. The weakly developed rachis appears to have formed through fusion of individual barbs that already possessed barbules (Stage IIIb), instead of fusion of naked barbs (Stage IIIa) [5]. The barb branching pattern continues largely uninterrupted toward the follicle, as do the pervasive, undifferentiated barbules. Unless the condition observed in DIP-V-15103 represents a secondary reduction of the rachis, the evolutionary pathway for feathers in this coelurosaur may have been through Stage IIIb (barbs with barbules), not Stage IIIa (fusion of naked barbs). Cytological observations of barbule development along the barb vane ridge support the evolutionary coupling of barbs and barbules [19,30]. Feather morphology of DIP-V-15103 contrasts with the reduced rachis and long, naked, filamentous barbs in the branched caudal plumage of the dromaeosaurid *Sinornithosaurus* [6,8] and the therizinosauroid *Beipiaosaurus* [31]. This either suggests a greater diversity of tail plumage in coelurosaurians than previously suspected, or a simplified form of more derived pennaceous feathers in DIP-V-15103.

The unusual barbule configuration in DIP-V-15103 suggests that barbules were primitively distributed evenly throughout the length of the feather and only later became restricted to the barbs and proximal rachis and oriented so that their edges face the feather surfaces, as in modern avians. In modern birds, barbule cells originate in the subperiderm and merge into a syncytium on either side of the barb vane ridge [32,33]. The symmetrical arrangement of barbules along the barbs in DIP-V-15103 implies symmetry of barbule cells across the barb vane ridge. The contiguous barbule branching along the rachis probably occurs along the barb vane ridge leading to the apicalmost barb. In the lineage leading to birds, the barbules became spatially restricted to the barbs and the proximal portion of the rachis, presumably to accommodate increasing barb number and density related to rigid pennaceous feathers (Stage IIIa+b and/or IV) [5]. Alternatively, the barbule pattern in DIP-V-15103 may represent a highly derived and potentially experimental character state unrelated to the avian lineage. Whichever the case, DIP-V-15103 suggests that non-avialan theropods had a greater variety of feather forms than predicted from developmental phenotypes in modern feathers [4,5,10].

Traces of pigmentation exist within the entombed plumage. Discrete bands corresponding to basal cells within each barbule are visible due to loosely confined pigments (Figure 3C–H). Pigmentation is more pronounced within apical portions of each barbule, and in the barb rami

and rachis of dorsal feathers (Figures 1C, S4H). Coloration varies little within individual feathers, but dorsal plumage is significantly darker than ventral plumage. Preserved coloration suggests a chestnut brown dorsal surface, contrasting against pale or almost white ventral plumage (Figures 1A–C, S4A–D); however, taphonomic impacts on visible colors are unclear. A small section of the pale ventral plumage was available for SEM observations. No melanosomes were observed, suggesting ventral plumage was either unpigmented or pigmented through alternative means, such as carotenoids [34]. Keratin sheets are visible within the feather layer, displaying the distinctive, porous, laminar structure also observed in modern avian barbules under SEM (Figure S2A,B).

The theropod tail reported here is an astonishing fossil, highlighting the unique preservation potential of amber. Importantly, in the context of bird origins, feathers and flight are key elements contributing to the success of the clade. Recent finds from Asia [1–4,6,8–11] have revealed unexpected diversity in feather morphologies and flight modes among the proliferation of small Jurassic–Cretaceous theropods near the origin of birds with powered flight. DIP-V-15103 adds another morphotype to this diversity. The integration of developmental studies [5,7,33] and paleontology yields enriched models of morphological character evolution that help explain major evolutionary transitions in key clades such as theropods, including birds. With preservation in amber, the finest details of feathers are visible in three-dimensions, providing concrete evidence for feather morphologies and arrangement upon the tail, and supporting an important role for barbs and barbules in feather evolution.

Experimental Procedures:

DIP-V-15103 was imaged and observed using propagation phase contrast Synchrotron Radiation X-ray microtomography (PPC-SR X-ray μCT); standard microscopy, micro- and macrophotography (including transmitted, incident, dark field, and UV lighting); and scanning electron microscopy (SEM). Chemical composition was analyzed using Synchrotron Radiation micro-X-ray fluorescence imaging (μ-XFI), and X-ray absorption spectroscopy (XAS). Full details of experimental procedures for imaging and chemical analyses are provided in Supplemental Experimental Procedures. Feather morphological terms follow [5] and [35], while pigmentation terminology follows [36]. Institutional abbreviations include DIP (Dexu Institute of

Palaeontology, Chaozhou, China); RSM (Royal Saskatchewan Museum, Regina, Canada). Specimen measurements are based on ocular micrometer readings, or 3-D reconstructions (with commentary).

Author Contributions:

L.X., R.M.: project design, leadership, funding, visualization, writing; X.X., W.P., T.M., P.C.: morphological analysis, editing; G.L., M.B., Q.Y.: 3D modeling, elemental analysis, editing; K.T.: taphonomic analysis; M.J.B., H.R.: data and CT model analysis, editing; J.Z.: geological background; A.W.: SEM analysis, editing.

Acknowledgments: We thank Chinese Academy of Science (YZ201211, BASIC 2014-01), National Science Fund of China (NSFC-J1210002), Shaanxi Province (No. 2013-19), National Geographic Society, USA (EC0768-15), National Sciences Engineering Research Council, Canada (2015-00681), and Humboldt Fellowship for support; Beijing Synchrotron Radiation Facility (BSRF) and Shanghai Synchrotron Radiation Facility (SSRF) for beamtime; staffs of 4W1A and B of BSRF, and 13W of SSRF, for analytical assistance; Zhao Haifei, Zhang Jie, An Pengfei and Wang Yanping of BSRF for research assistance; Ray Poulin (RSM) for discussions; and Nathan Gerein (University of Alberta) for SEM assistance.

References:

1. Ji, Q., and Ji, S-A. (1996). On the discovery of the earliest fossil bird in China (*Sinosauropteryx* gen. nov.) and the origin of birds. Chin. Geol. 233, 30–33.
2. Ji, Q., Currie, P.J., Norell, M.A., and Ji, S. (1998). Two feathered dinosaurs from northeastern China. Nature 393, 753–761.
3. Chen, P.J., Dong, Z.M., and Zhen, S.N. (1998). An exceptionally well-preserved theropod dinosaur from the Yixian Formation of China. Nature 391, 147–152.
4. O'Connor, J.K., Chiappe, L.M., Chuong, C., Bottjer, D.J., and You, H. (2012) Homology and potential cellular and molecular mechanisms for the development of unique feather morphologies in early birds. Geosciences 2, 157–177.

5. Prum, R.O. (1999) Development and evolutionary origin of feathers. J. Exp. Zool. 285, 291–306.
6. Xu, X., Zhou, Z., and Prum, R.O. (2001). Branched integumental structures in *Sinornithosaurus* and the origin of feathers. Nature 410, 200–204.
7. Prum, R.O., and Dyck, J. (2003). A hierarchical model of plumage: morphology, development, and evolution. J. Exp. Zoolog. B Mol. Dev. Evol. 298B, 73–90.
8. Xu, X., Zheng, X., and You, H. (2010). Exceptional dinosaur fossils show ontogenetic development of early feathers. Nature 464, 1338–1341.
9. Xu, X., *et al.* (2014). An integrative approach to understanding bird origins. Science 346, 1253293.
10. Chen, C.-F., *et al.* (2015). Development, regeneration, and evolution of feathers. Annu. Rev. Anim. Biosci. 3, 169–195.
11. Norell, M.A., and Xu, X. (2005). Feathered dinosaurs. Annu. Rev. Earth. Planet. *Sci.* 33, 277–299.
12. McKellar, R.C., Chatterton, B.D.E., Wolfe, A.P., and Currie, P.J. (2011). A diverse assemblage of Late Cretaceous dinosaur and bird feathers from Canadian amber. Science 333, 1619–1622.
13. Nascimbene, P.C., Dove, C.J., Grimaldi, D.A., and Schmidt, A.R. (2014). Exceptional preservation of feather microstructures in amber from diverse faunas (Theropoda: Paraves) during the Lower and mid-Cretaceous. 9th European Palaeobotany-Palynology Conference, Pavoda, Italy Abstract Book pp. 113–114.
14. Xing, L. et al. (2016). Mummified precocial bird wings in mid-Cretaceous Burmese amber. Nat. Comm. 7(12089), doi: 10.1038/ncomms12089
15. Schlee, D., and Glöckner, W. (1978). Bernstein: Bernsteine und Bernstein-Fossilien. Stuttg. Beitr. Naturkd. *C* 8, 1–72.
16. Grimaldi, D.A., and Case, G.R. (1995). A feather in amber from the Upper Cretaceous of New Jersey. Am. Mus. Novit. 3126, 1–6.
17. Grimaldi, D.A., Engel, M.S., and Nascimbene, P.C. (2002). Fossiliferous Cretaceous amber from Myanmar (Burma): its rediscovery, biotic diversity, and paleontological significance. Am. Mus. Novit. 3361, 1–72.
18. Perrichot, P., Marion, L., Néraudeau, D., Vullo, R., and Tafforeau, P. (2008). The early

306 evolution of feathers: fossil evidence from Cretaceous amber of France. Proc. R. Soc. B 275,
307 1197–1202.
308 19. Alibardi, L. (2006). Cells of embryonic and regenerating germinal layers within barb ridges:
309 implication for the development, evolution and diversification of feathers. J. Submicrosc.
310 Cytol. Pathol. 38, 51–76.
311 20. De Queiroz, K., Chu, L.-R., and Losos, J.B. (1998) A second *Anolis* lizard in Dominican
312 amber and the systematics and ecological morphology of Dominican amber anoles. Am.
313 Mus. Novit. 3249, 1–23.
314 21. Schweitzer, M.H., *et al.* (2014). A role for iron and oxygen chemistry in preserving soft
315 tissues, cells and molecules in deep time. Proc. R. Soc. B 281, 20132741.
316 22. Grimaldi, D.A., and Engel, M.S. (2005). Evolution of the Insects (Cambridge Univ. Press).
317 23. Colleary, C. *et al.* (2015). Chemical, experimental, and morphological evidence for
318 diagenetically altered melanin in exceptionally preserved fossils. PNAS 112(41), 12592–
319 12597.
320 24. O'Connor, J.K., Wang X., Zheng X., Hu H., Zhang X., and Zhou Z. (2016). An
321 enantiornithine with a fan-shaped tail, and the evolution of the rectricial complex in early
322 birds. Current Biol. 26(1), 114-119.
323 25. Zhang, F., Zhou, Z., Xu, X., Wang, X., and Sullivan, C. (2008) A bizarre Jurassic
324 maniraptoran from China with elongate ribbon-like feathers. Nature 455, 1105–1108.
325 26. O'Connor, J.K., and Zhou, Z. (2013). A redescription of *Chaoyangia beishanensis* (Aves)
326 and a comprehensive phylogeny of Mesozoic birds. J. Syst. Palaeontol. 11, 889–906.
327 27. Persons, W.S., Currie, P.J., and Norell, M.A. (2013). Oviraptorosaur tail forms and functions.
328 Acta Palaeontol. Pol. 59, 553–567.
329 28. Currie, P.J., and Chen, P. (2001). Anatomy of *Sinosauropteryx prima* from Liaoning,
330 northeastern China. Can. J. Earth Sci. 38, 1705–1727.
331 29. O'Connor, J.K., Sun, C., Xu, X., Wang, X., and Zhou, Z. (2012). A new species of *Jeholornis*
332 with complete caudal integument. Hist. Biol. 24, 29–41.
333 30. Alibardi, L., and Sawyer, R.H. (2006). Cell structure of developing downfeathers in the
334 zebrafinch with emphasis on barb ridge morphogenesis. J. Anat. 208, 621–642.
335 31. Xu, X., Tang, Z., and Wang, X. (1999). A therizinosauroid dinosaur with integumentary
336 structures from China. Nature 399, 350.

32. Alibardi, L. (2005). Cell structure of developing barbs and barbules in downfeathers of the chick: central role of barb ridge morphogenesis for the evolution of feathers. J. Submicrosc. Cytol. Pathol. 37, 19–41.
33. Alibardi, L. (2007). Cell interactions in barb ridges of developing chick downfeather and the origin of feather branching. Ital. J. Zool. 74, 143–155.
34. Thomas, D.B., Nascimbene, P.C., Dove, C.J., Grimaldi, D.A., and James, H.F. (2014). Seeking carotenoid pigments in amber-preserved fossil feathers. Sci. Rep. 4, 10.1038/srep05226.
35. Lucas, A.M., and Stettenheim, P.R. (1979). Avian Anatomy: Integument (Washington: US Gov. Printing Office).
36. Dove, C.J. (2000). A descriptive and phylogenetic analysis of plumulaceous feather characters in Charadriiformes. Ornithol. Monogr. 51, 1–163.

Figure 1. Photomicrographs and SR X-ray μCT reconstructions of DIP-V-15103. **(A)** Dorsolateral overview. **(B)** Ventrolateral overview with decay products (bubbles in foreground, staining to lower right). **(C)** Caudal exposure of tail, showing darker dorsal plumage (top), milky amber, exposed carbon film around vertebrae (center). **(D–H)** Reconstructions focussing on dorsolateral, detailed dorsal, ventrolateral, detailed ventral, and detailed dorsal aspects of tail, respectively. Arrowheads in (A), (D) mark rachis of feather featured in Figure 4A. Asterisks in (A) and (C) indicate carbonized film (soft tissue) exposure. Arrows in (B), (E–G) indicate shared landmark, plus bubbles exaggerating rachis dimensions; brackets in (G) and (H) delineate two vertebrae with clear transverse expansion and curvature of tail at articulation. Abbreviations for feather rachises: d, dorsal; dl, dorsalmost lateral; vl, ventralmost lateral; v, ventral. Scale bars 5 mm in A,B,D,F; 2 mm in C,E,G,H. See also Figure S2.

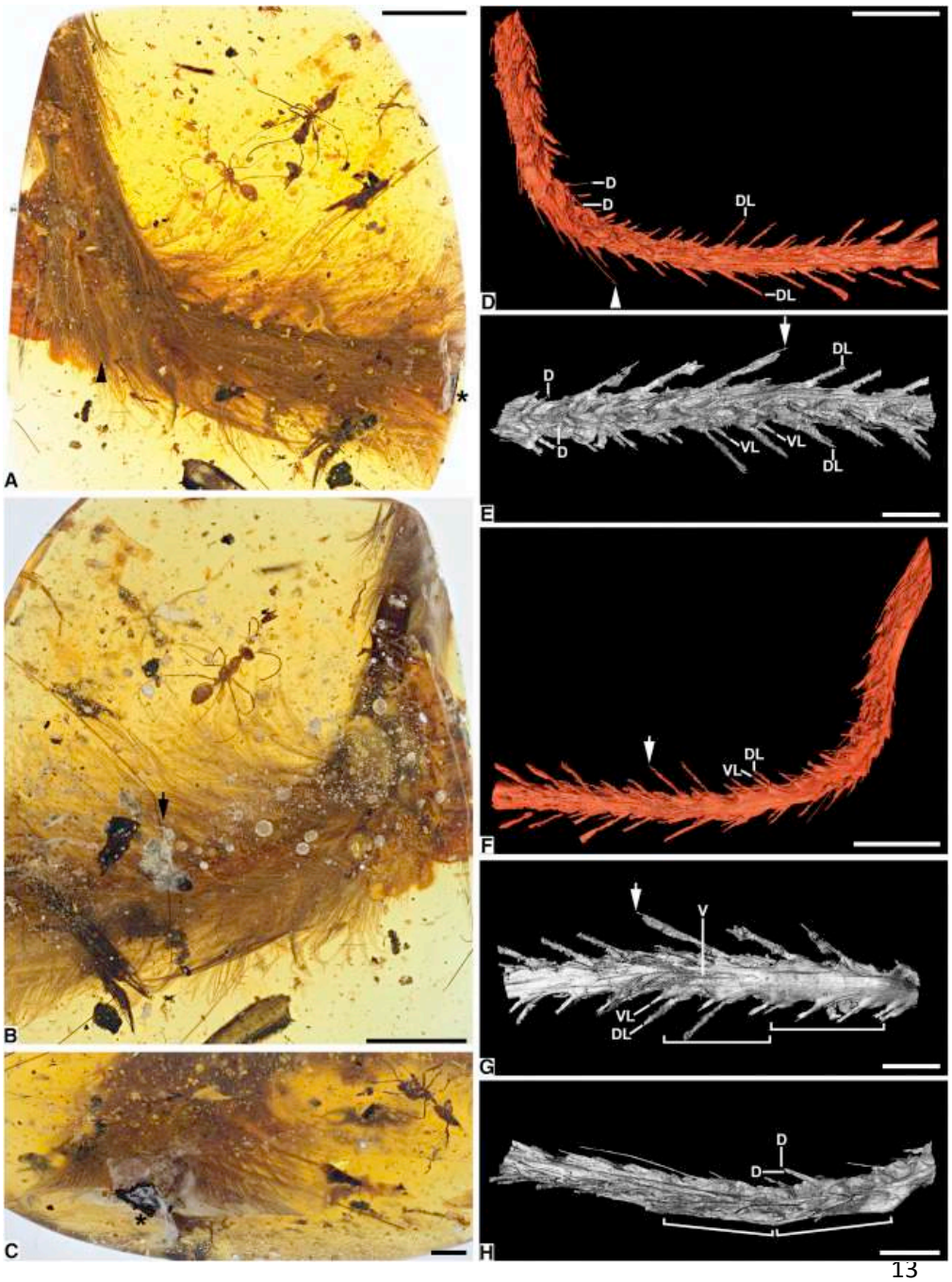

Figure 2. SR μ-XFI maps and scanning electron micrographs of DIP-V-15103. **(A)** Elemental maps and ROI image for exposed soft tissue preservation in DIP-V-15103; black carbon film surrounds clay minerals infilling void between vertebrae or partially replacing them; milky amber related to decay surrounds vertebrae and plumage (ROI prior to clay flake removal better visible in Figure S3H). **(B)** Patchy keratin preservation with traces of fibrous structure in DIP-V-15103 ventral feather. **(C)** Fibrous keratin sheets and isolated melanosomes from barb of modern Indian peafowl (*Pavo cristatus*; Galliformes). Scale bars = 2 mm in A; 1 μm in B,C. See also Figure S3.

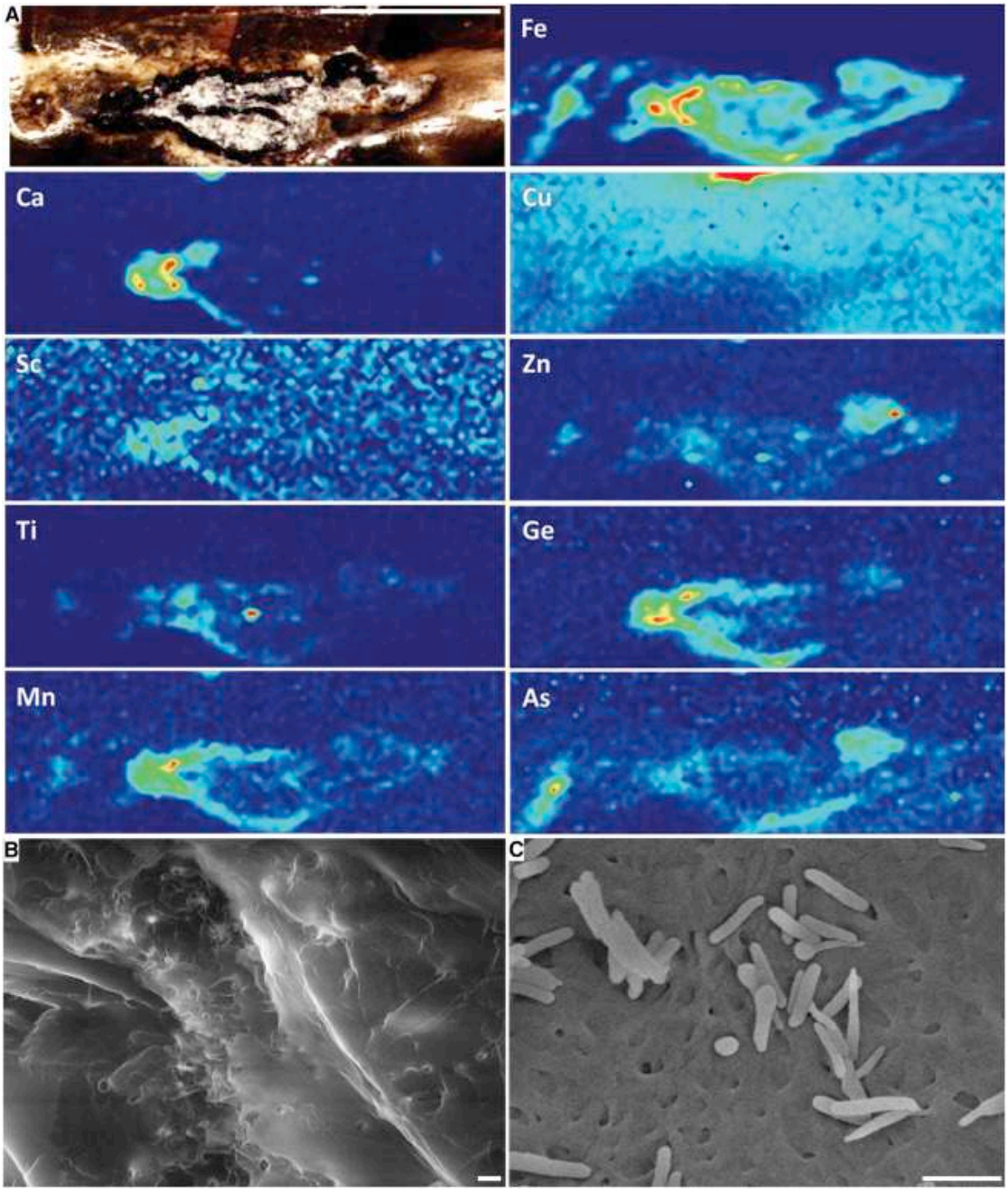

Figure 3. Photomicrographs of DIP-V-15103 plumage. **(A)** Pale ventral feather in transmitted light (arrow indicates rachis apex). **(B)** Dark field image of (A), highlighting structure and visible color. **(C)** Dark dorsal feather in transmitted light, apex toward bottom of image. **(D)** Base of ventral feather (arrow) with weakly developed rachis. **(E)** Pigment distribution and microstructure of barbules in (C), with white lines pointing to pigmented regions of barbules. **(F-H)** Barbule structure variation and pigmentation, among barbs, and 'rachis' with rachidial barbules (near arrows); images from apical, mid-feather, and basal positions respectively. Scale bars = 1 mm in A, 0.5 mm in B–E, 0.25 mm in F-H. See also Figure S4.

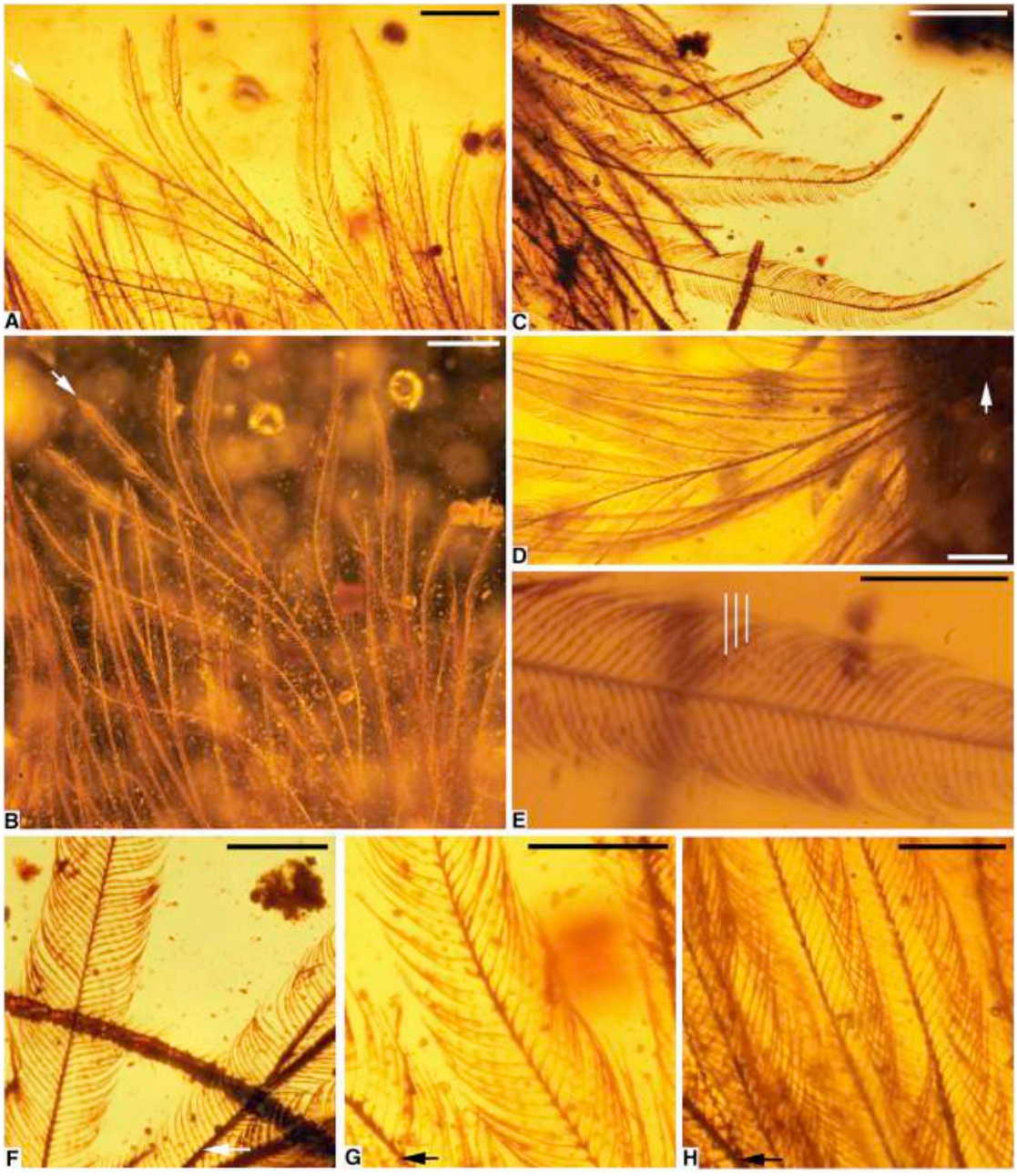

Figure 4. DIP-V-15103 structural overview, and feather evolutionary-developmental model fit. **(A,B)** Overview of largest and most planar feather on tail (dorsal series, anterior end), with matching interpretive diagram of barbs and barbules. Barbules omitted on upper side and on one barb section (near black arrow) to show rachidial barbules and structure; white arrow indicates follicle. **(C)** Evolutionary-developmental model and placement of new amber specimen. Brown = calamus, blue = barb ramus, red = barbule, purple = rachis [after 5, 12]. Scale bars = 1 mm in A,B.